Cell Biochem Biophys (2015) 71:1463–1473
DOI 10.1007/s12013-014-0369-7

ORIGINAL PAPER

Transplantation of iPSc Restores Cardiac Function by Promoting Angiogenesis and Ameliorating Cardiac Remodeling in a Post-infarcted Swine Model

Guixian Song · Xiaorong Li · Yahui Shen · Lingmei Qian · Xiangqing Kong · Minglong Chen · Kejiang Cao · Fengxiang Zhang

Published online: 12 November 2014
© Springer Science+Business Media New York 2014

Abstract Induced pluripotent stem cells (iPSc) hold significant promise for the development of cardiac regenerative therapy for myocardial infarction (MI). However, preclinical optimization and validation of large-animal models will be required before iPSc used clinically. Therefore, we aim to investigate the therapeutic potential of iPSc transplantation for MI and relative mechanisms in a post-infarcted swine model. Left anterior descending coronary artery was balloon-occluded after percutaneous transluminal angiography to generate MI (60-min no-flow ischemia). Animals were then divided into Sham, PBS control, and iPS experimental groups. The cardiac function and LV structural were assessed by dual-source computed tomography. Terminal deoxynucleotidyl nick end labeling, histology, and immunofluorescence were used to examine the effect of transplanted iPS cells on apoptosis, fibrosis, and hypertrophy. At 6 weeks, LV structural abnormality and cardiac dysfunction were less pronounced in iPSc group than in PBS group, and these improvements were accompanied by reduction of scar size. iPSc transplantation was associated with significant increase of vascular density and reduced myocardial apoptosis in the border zone of infarction, which was accompanied by the reduction in fibrosis degree. Moreover, proangiogenic and antiapoptotic factors were increased significantly in iPS group compared with PBS group. Cardiomyocyte hypertrophy was significantly attenuated by iPSc transplantation. In conclusion, these results suggested that transplantation of iPSc may result in functional recovery by promoting angiogenesis, inhibiting apoptosis, and ameliorating cardiac remodeling. This proof of concept study may provide a basis for an autologous iPSc-based therapy of MI.

Keywords Induced pluripotent stem cell · Myocardial infarction · Cardiac remodeling · Apoptosis · Fibrosis

Introduction

Cardiovascular disease leading to myocardial infarction (MI) affects a large population, with occurrence of acute coronary blockage causing irreversible myocardial damage, morbidity, and mortality [1]. MI may lead to congestive heart failure implicated by multiple mechanisms such as cardiac myocyte apoptosis, hypertrophy, and fibrosis [2, 3]. Unfortunately, current therapeutic interventions to inhibit further deterioration of MI leading to end stage heart failure are rather limited. It is widely accepted that cardiac myocytes do not regenerate due to lack of a substantive pool of precursor, stem, or reserve cells in adult hearts. Moreover, donor heart for transplantation required to manage end stage heart failure patients is not readily available [4]. Therefore, new cellular therapies to repair and regenerate injured myocardium, as well as to prevent the progression of a diverse cardiac remodeling are under active investigation.

Guixian Song, Xiaorong Li and Yahui Shen have contributed equally to this work.

G. Song · X. Li · L. Qian · X. Kong · M. Chen · K. Cao (✉) · F. Zhang (✉)
Department of Cardiology, The First Affiliated Hospital of Nanjing Medical University, Nanjing 210029, China
e-mail: kejiangcao@163.com

F. Zhang
e-mail: njzfx6@163.com

Y. Shen
State Key Laboratory of Reproductive Medicine, Nanjing Maternity and Child Health Care Hospital Affiliated to Nanjing Medical University, Nanjing 210029, China

Traditional stem cell therapies face various impediments, including the typical ethical and immunological problems in clinical application. Recently, induced pluripotent stem (iPS) cells have been shown to offer a novel attractive route to patient-specific and disease-specific pluripotent cells, without the technical and ethical limitations of somatic cell nuclear transfer method [5, 6]. These induced pluripotent stem cells (iPScs) are essentially identical to embryonic stem cells (ESCs), but offer the possibility to generate autologous patient-specific pluripotent stem cells. It has been shown that murine and human iPScs are able to form multipotent cardiovascular progenitors and mature cardiomyocytes similar to those derived from ESCs [7–10].

With regard to the potential therapeutic application of pluripotent stem cell derivatives, great progress has been achieved concerning scalable cell production and more efficient and specific differentiation into target cell types [11, 12]. The potential therapeutic benefits of iPSc-based cell treatment for MI have been confirmed in vitro or in proper small animal models [13–15]. However, clinical application of iPSc will require further preclinical exploration and validation in large-animal models, which are more similar to humans. The pig, as the common livestock, not only resembles the human in heart dimension, structure, and function, but also is similar in immunological and physiological characteristics. Thus, in the present study, we established a post-infarction swine model and injected piPSc into injured myocardium to test the hypothesis that this novel cell-based therapy can exert a cardioprotective effect after MI and further investigate the possible mechanism.

Materials and Methods

Animals

Two-month-old Suzhong swines (25 ± 5 kg) were obtained from the Nanjing Academy of Agricultural Sciences. All experimental procedures were performed in accordance with the Guide for the Care and Use of Laboratory Animals published by the US National Institutes of Health and were approved by the Experimental Animal Ethics Committee of Nanjing Medical University, China.

Cell Line and Cell Culture

iPS cells were kindly provided by professor Lei Xiao (Shanghai Institutes for Biological Sciences, Chinese Academy of Sciences, China). This porcine iPSc line was derived from primary ear fibroblasts or primary bone marrow cells of 10-week-old Danish Landrace pigs by drug-inducible expression of defined factors including Oct4, Sox2, Klf4, c-Myc, Nanog, and Lin28. This iPSc line has been proven to differentiate into three germ layers in vitro and in vivo. Cell culture methods and basic features of iPSc have been detailed by Zhao et al. [16]. iPSc was transduced with adenovirus expressing the enhanced green fluorescent protein (GFP) reporter gene and cultured on irradiated mouse embryonic fibroblasts.

Establishment of Myocardial Infarction Models

The MI models were established as described previously [17]. Following the successful establishment of the models, mini-swines ($n = 18$) were randomly allocated to three groups as follows:

Sham group ($n = 6$): Coronary angiography but without Left anterior descending (LAD) occlusion;

PBS group ($n = 6$): LAD occlusion followed by phosphate buffer solution (PBS) injection after one week; and

iPS group ($n = 6$): LAD occlusion followed by iPSc transplantation after one week.

iPScs Transplantation

One week after MI induction, an open-chest operation was carried out for cell transplantation. The infarcted region was identified by color change from bright red to dark blue and abnormal wall motion. The porcine in iPS group received intramyocardial injection of 2×10^7 porcine iPS cells suspended in 2 ml of sterile PBS solution both in the center of the infarct zone (IZ) for 10 sites and along the border zone (BZ) for 10 sites (0.1 ml per injection, 1×10^6 cells per site). Same volume PBS was injected into the corresponding sites in the PBS group. Haemostasis was performed and the chest was closed in layers. Post-operatively, penicillin G benzathine (30,000 U/day) was administered intravenously for 3 days. In addition, cyclosporine and methyleneprednisolone were injected intramuscularly for 2 weeks in the iPS and PBS group as previously [11], which help to alleviate the non-specific immune response and the acute inflammatory reactions.

Assess of Cardiac Function and LV Structure by DSCT

A 64-slice Dual-source computed tomography (DSCT, Somatom Definition, Siemens Healthcare, Germany) was performed to determine the cardiac function and structure at baseline, the first and sixth weeks after MI model establishment. The DSCT scan protocol and image reconstruction described as our previous study [18] were used to assess cardiac performance. At the end of each study, the heart was removed and sectioned from the occlusion location of the apex into five transverse slices in a plane

parallel to the atrioventricular groove. The left ventricular (LV) sections were divided into three portions as described by Zhang et al. [19]: the infarct zone, defined as a myocardial region devoid of myocytes; the peri-infarct region, the region 2 cm away from the infarct zone; and the distant region, the region 5 cm away from the infarction.

Detection of Apoptosis by TUNEL Assay

Tissue frozen sections that already prepared from corresponding zone were taken from ultra deep-freeze equipment and fixed with acetone for 10 min. Myocardial apoptosis was analysed by TUNEL (terminal deoxynucleotidyl transferase dUTP nick end labeling) assay using an in situ cell death detection kit (Roche Molecular Biochemicals, Mannheim, Germany). TUNEL staining for apoptotic cell nuclei and 4, 6-diamino-2-pheny indole staining for all myocardial cell nuclei as described previously [20]. The percentage of apoptotic nuclei per section was calculated by counting the total number of TUNEL-staining nuclei divided by the total number of DAPI-positive nuclei.

Measurement of Infarct Size and Fibrosis

Infarct size was determined with planar morphometry in triphenyltetrazolium chloride (TTC) (Sigma Chemicals, St. Louis, MO, USA) stained sections and expressed as a ratio of the left ventricular area. Each heart was removed and sliced horizontally into 4 mm slices, which were incubated in 1 % TTC in phosphate-buffered saline at 37 °C for 5 min and fixed for 12 h in 10 % phosphate-buffered formalin. Both sides of each slice were photographed with a digital camera. The boundary of the unstained area (infarcted tissue) was traced in a blinded fashion and quantified with dedicated software (Image J). The sections were then washed repeatedly with PBS, processed, and embedded in paraffin for hematoxylin-eosin (H&E) and Masson trichrome staining to assess fibrosis in the infracted and peri-infarcted myocardium. Fibrosis area and total area of each image were measured by computerized planimetry(Image ProPlus, Media Cybernetics, SilverSpring, MD), and the percentage of the fibrosis was calculated as follows: (fibrosis area/total area) $\times$ %.

Western Blot Analysis

At 6 weeks after MI, pulverized frozen samples from the BZ of infarction were analyzed by quantitative immunoblotting using antibodies against vascular endothelial growth factor (VEGF; Sigma-Aldrich), interleukin-1 (IL-1; Santa Cruz), interleukin-6 (IL-6; Santa Cruz), Bax (Santa Cruz), and B cell lymphoma 2 (Bcl-2; Santa Cruz). The protein concentrations of the samples were determined by the BCA method. Proteins (50 μg) were resolved by 14 % sodium dodecyl sulfate polyacrylamide gel electrophoresis (SDS-PAGE) and transferred to a PVDF membrane. Primary antibody was added after blocking the membrane and incubated with the membrane overnight at 4 °C. The housekeeping protein GAPDH was used as an internal standard. Horseradish peroxidase-linked secondary antibodies (Zhongshan Golden Bridge) were used, and proteins were visualized by an ECL kit. The bands were then exposed to radiography film, followed with densitometric quantification by image J software analysis.

Immunofluorescence Analysis

The transplanted iPScs had been engineered to express GFP; thus, the survival and differentiation of transplanted iPScs were evaluated by staining for the co-expression of GFP, α-actin, and vWF. The distribution of the GFP-positive cells suggested the survival of transplanted cells. In addition, the vascularization and transdiameter of cardiomyocyte were also evaluated by immunofluorescence staining. The following antibodies were used for these experiments: mouse anti-SMA(smooth muscle actin) (San Francisco, CA, USA), rabbit anti-von Willebrand factor (vWF; Sigma-Aldrich), and α-actin (Sigma-Aldrich). Samples from the BZ or a corresponding zone of the Sham group taken from liquid nitrogen were embedded immediately into an optimal cutting temperature compound (Miles-Bayer) and cut into 5-μm sections. The slices were rinsed and then incubated with the primary antibody at 4 °C overnight. The next day, the slices were rinsed five times and incubated prior to the addition of secondary antibody. The slices were coded so that the investigator was blinded to the identification of the pig sections. Vessel density was expressed as the number of SMA positives per square millimeter. Under a fluorescence microscope, the vessel density counts in each group were averaged from 30 fields (six slides and five areas in each slide). Adopting the similar method, cardiomyocytes diameter was calculated using the Image J Software.

Statistical Analysis

Continuous variables were expressed as mean $\pm$ standard deviation (SD). Each experiment was performed at least three times independently. The data are analyzed by the Student's *t* test or one-way analysis of variance (ANOVA) test, Kruscal–Wallis *H* tests and Mann–Whitney *U* tests were used when the data were not met the normal distribution criteria or homogeneity of variance using the SPSS 13.0 software (SPSS, Chicago, II, USA). Categorical variables were presented as percentage ratio and compared

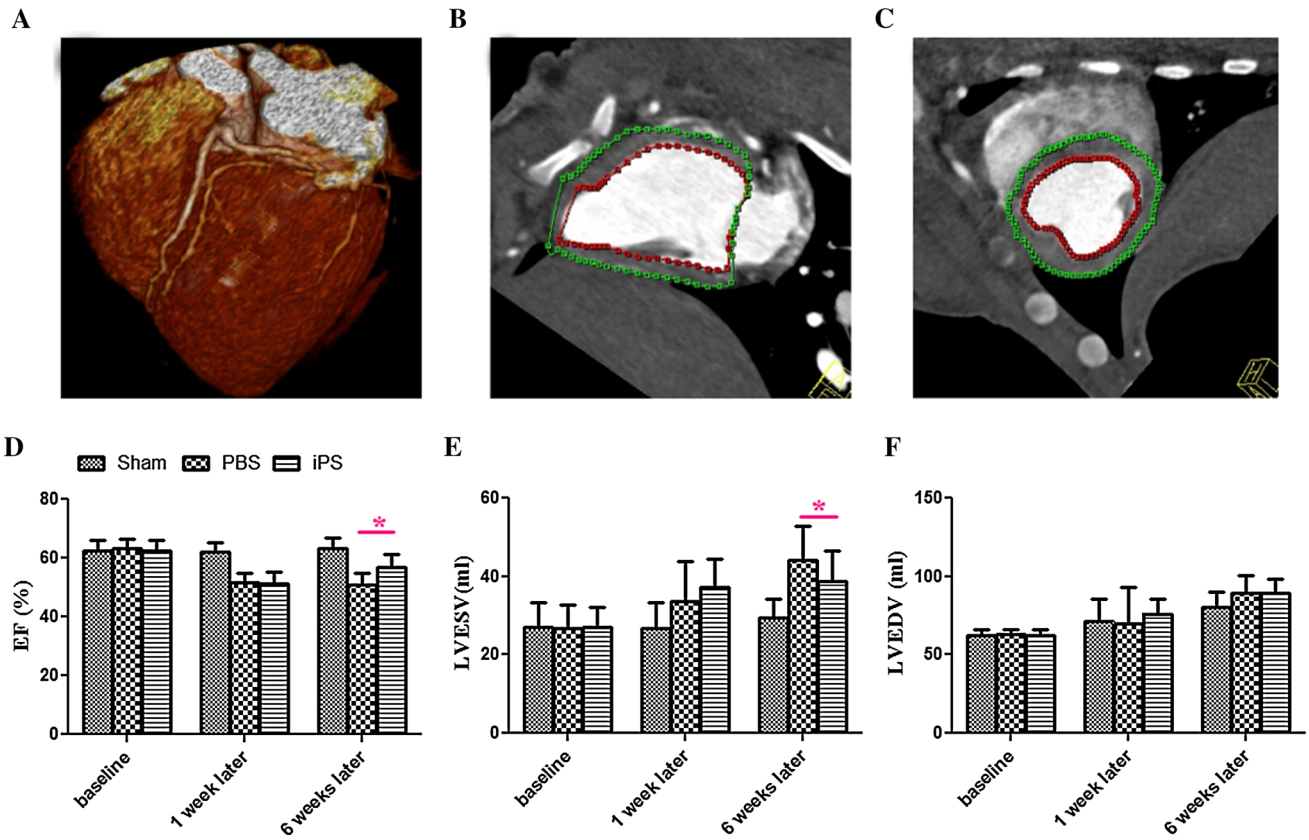

Fig. 1 Structural and functional benefits of iPSc transplantation. Heart overall view of DSCT images (**a**). Representative cardiac DSCT images at end systole and end diastole (**b**, **c**). At baseline, no significant differences in DSCT parameters were found among the groups. At end point, MI injury led to a significant decline in LVEF, while the iPS group showed a significantly improvement in LVEF (**d**). In addition, the change in ESV was significant in comparison between the iPS-treated hearts and the PBS-treated hearts, indicating that the systolic function of the left ventricle was remarkably improved by iPSc transplantation (**e**). However, the change in EDV was not significantly different among the groups (**f**). *iPS group vs. PBS group, $P < 0.05$. *LVEF* LV ejection fraction, *EDV* end-diastolic volume, *ESV* end-systolic volume

by χ^2 test unless otherwise indicated. $P < 0.05$ was considered to be significant.

Results

iPSc Transplantation Improved Cardiac Performance and Reduced LV Remodeling after MI

Typical cardiac DSCT images of heart at end diastole and end systole are shown in Fig. 1a–c. Serial DSCT analysis indicated that the baseline parameters were similar in all groups (Fig. 1d–f). 6 weeks later, MI injury led to a significant decline in left ventricle ejection fraction (LVEF), while the iPS transplantation showed a significantly improvement in LVEF (Fig. 1d). Moreover, the change in end-systolic volume (ESV) was significant in comparison between the iPS group and the PBS group (Fig. 1e); indicating that the systolic function of the left ventricle was remarkably improved by iPSc transplantation. However, the change in end-diastolic volume (EDV) was not significantly different among the groups (Fig. 1f).

Survival and Engraftment of iPSc in Infarcted Swine Heart

The transplanted iPSc had been engineered to express GFP; thus, the survival and differentiation of transplanted iPSc were evaluated by double staining for the expression of GFP, α-actin, and vWF. The distribution of the GFP-positive cells suggested the survival of transplanted cells. As a result, frozen sections showed GFP-positive cells distributed in all regions in the iPS group, whereas most transplanted cells were found in the border zone. However, only in a few regions, the GFP-positive spots were coincident with the red fluorescence spots of the α-actin antibody (Fig. 2a), suggesting iPSc hardly survive as myoblasts. However, in many regions, the GFP-positive spots were coincident with the red fluorescence spots of the vWF antibody(Fig. 2b), suggesting transplanted iPSc appeared to differentiated into vascular

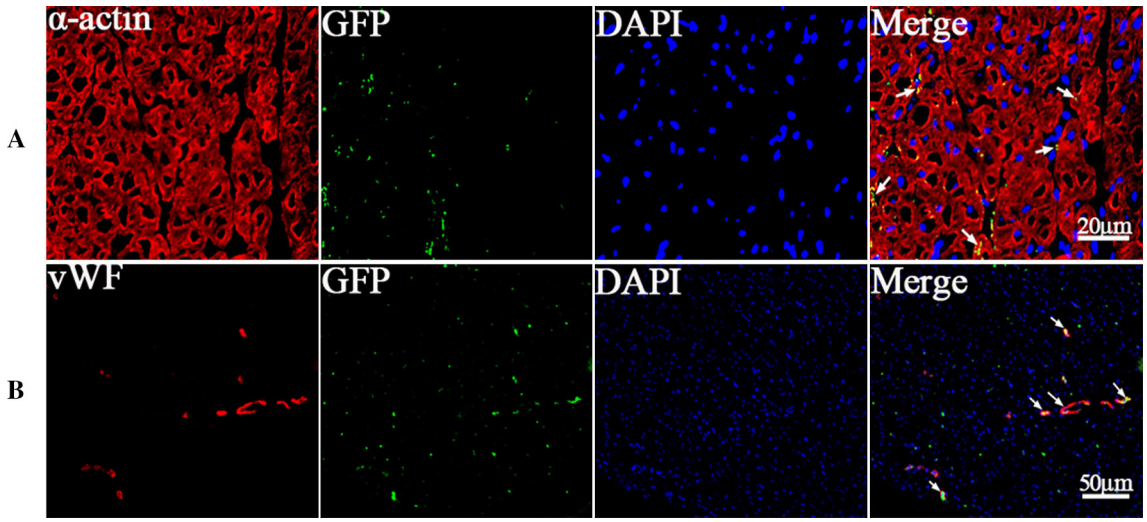

Fig. 2 The fate of engrafted iPSc. The *arrows* designate the engraftment area of the iPSc. Surviving iPSc were immunostained for actin with a *red fluorescent marker*. The coexistence of GFP and actin was found only on a small scale, demonstrating that there was no obvious cardiomyogenic differentiation 6 weeks after transplantation (**a**). 6 weeks after cell transplantation, double-label immunofluorescence staining indicated that the iPSc can survive in the BZ of infarction and have the tendency to differentiate into vascular endothelial cells. *Yellow fluorescence* indicates colocalization of immunofluorescent antibodies vWF (*red*) and GFP (*green*) (**b**). Magnification, ×400 for **a**, ×200 for **b** (Color figure online)

endothelial cell, or integrate into pre-existing vessels and to generate new vessel (our data cannot distinguish exactly).

iPSc Transplantation Limited Infarct Size and Attenuated Inflammatory Response

The effect of iPSc intramyocardial injection on myocardial injury 6 weeks after infarction was evaluated by TTC staining (Fig. 3a–c). Mean infarct size in the PBS-treated hearts was 15.98 ± 1.57 % of the LV, in contrast, injection of iPSc had a significant protective effect, limiting the size of the infarct to 12.04 ± 1.46 % of the LV, which may be responsible for the improvement in cardiac function (Fig. 3g).

In addition, the inflammatory response was evaluated by H&E staining. There were massive infiltrations of inflammatory cells in PBS-treated hearts; treatment with iPSc remarkably attenuated the inflammatory response (Fig. 3d–f). Meanwhile, the expression level of IL-1 and IL-6 was significantly reduced in iPSc-treated hearts compared to PBS group (Fig. 3h, i).

Vascularization and Expression of VEGF

To determine the mechanisms underlying the beneficial effects of iPSc transplantation, we investigated the effects of iPSc transplantation on angiogenesis in the post-MI hearts. At 6 weeks post-cell transplantation, immunofluorescence staining for SMA antibody indicated significant angiogenesis in iPSc-treated hearts, with more SMA-expressing vessels being present in the iPSc-treated hearts compared with the PBS-treated hearts, whether in IZ or BZ (Fig. 4a). Quantitative evaluation of the numbers of SMA-positive vessels per high-power field (20×) indicated that the vascular density was significantly greater in the iPSc-treated hearts than in the PBS-treated hearts (* iPS-IZ 14 ± 3/field vs. PBS-IZ 10 ± 2/field; # iPS-BZ 26 ± 4/field vs. PBS-BZ 18 ± 3/field; $P < 0.05$) (Fig. 4c). To further identify angiogenic factors, we calculated the levels of VEGF. Western blot analysis demonstrated that the expression levels of VEGF in the iPS-treated heart were significantly higher than the PBS-treated hearts at six weeks after cell transplantation (Fig. 4b, d).

iPSc Transplantation Inhibited Myocardial Apoptosis

As shown in Fig. 5a, there was no significant difference between the percentage of TUNEL-positive cardiomyocytes in iPS-IZ and PBS-IZ. However, MI-related apoptosis was significantly increased in the PBS-BZ compared with Sham heart, and this effect after MI was remarkably attenuated in iPS-BZ. The graphs show quantitative analyses for total TUNEL-positive cells in different regions of all groups (# iPS-BZ 10.3 ± 2.3 % vs. PBS-BZ 15.6 ± 1.8 %; $P < 0.05$) (Fig. 5b).

To investigate the underlying molecular mechanism of the antiapoptotic effects of iPS transplantation, we examined expression of the Bcl-2 protein family by Western blot analysis. The results indicated that the proapoptotic protein Bax was significantly increased in PBS-treated hearts after

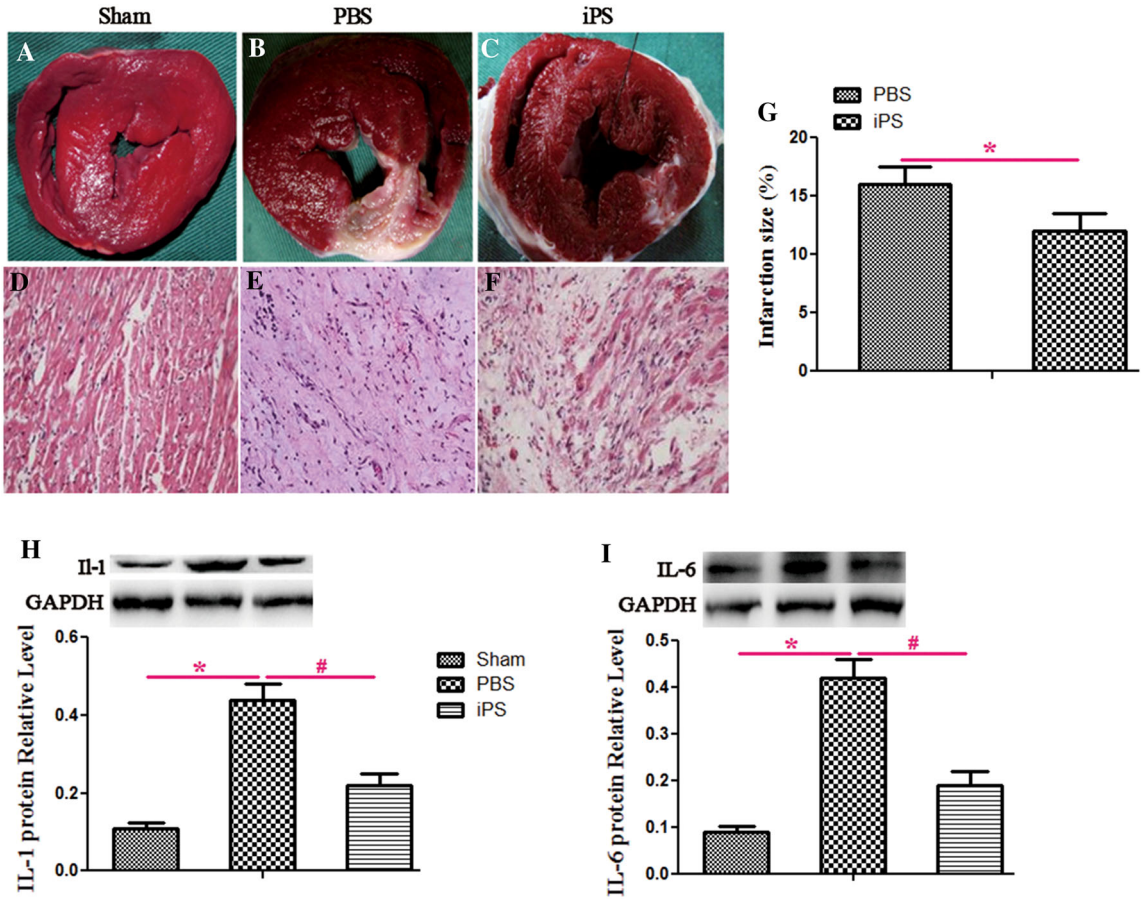

Fig. 3 Effect of the iPSc on infarct size and inflammatory response. The LAD occlusion in the PBS control group resulted in a large infarct size (**b**), after injection of iPSc, infarct size was reduced significantly (**c**). Massive infiltration of inflammatory cells can be seen in PBS-treated hearts compared to Sham hearts (**d**, **e**); iPS transplantation remarkably attenuated the inflammatory response (**f**). Quantitative analysis of infracted area using Image Proplus (**g**) (*iPS group vs. PBS group, $P < 0.05$). Meanwhile, the expression level of IL-1 and IL-6 was significantly reduced in iPSc-treated hearts compared to PBS-treated hearts (**h**, **i**). *PBS vs. Sham; #iPS vs. PBS ($P < 0.05$)

MI compared with Sham swine, whereas the expression of proapoptotic proteins was significantly decreased in iPS-treated hearts, whether in IZ or BZ (Fig. 6a, c). However, the expression of antiapoptotic proteins Bcl-2 was significantly increased in the iPSc-treated hearts compared with the PBS-treated hearts in BZ (Fig. 6b, d).

iPSc Transplantation Attenuates Myocardial Hypertrophy and Reduces Fibrosis

To determine the effect of iPSc transplantation on cardiomyocyte hypertrophy, we measured cardiomyocyte transdiameter. Typical pictures of double immunofluorescence staining using α-actin and DAPI are shown in Fig. 7a. The PBS-BZ demonstrated a significant increase in cardiomyocyte diameter (μm) in the peri-infarct regions of the heart compared with Sham group, but iPS transplantation significantly alleviated the cardiomyocyte hypertrophy(# iPS-BZ 15.2 ± 0.6 μm vs. PBS-BZ 20.4 ± 0.7 μm; $P < 0.05$) (Fig. 7b). In addition, we calculated the ratio of the whole heart weight (WHW) to body weight (BM), the results showed that the WHW/BW in PBS group was significantly higher than Sham group, whereas the ratio was less in iPS group compared to PBS group (# iPS group 11.2 ± 1.6 g/kg vs. PBS group 13.2 ± 1.8 g/kg; $P < 0.05$) (Fig. 7c), thus, further confirmed that iPSc transplantation attenuated myocardial hypertrophy.

To determine the effect of transplanted iPSc on cardiac fibrosis, we quantified the fibrotic area in the myocardial sections. The iPS-treated hearts demonstrated less fibrosis compared with the PBS-treated hearts whether in IZ or BZ (*iPS-IZ 40.2 ± 3.1 % vs. PBS-IZ 50.6 ± 10.2 %; # iPS-BZ 2.4 ± 0.6 % vs. PBS-BZ 6.1 ± 1.2 %; $P < 0.05$) (Fig. 8).

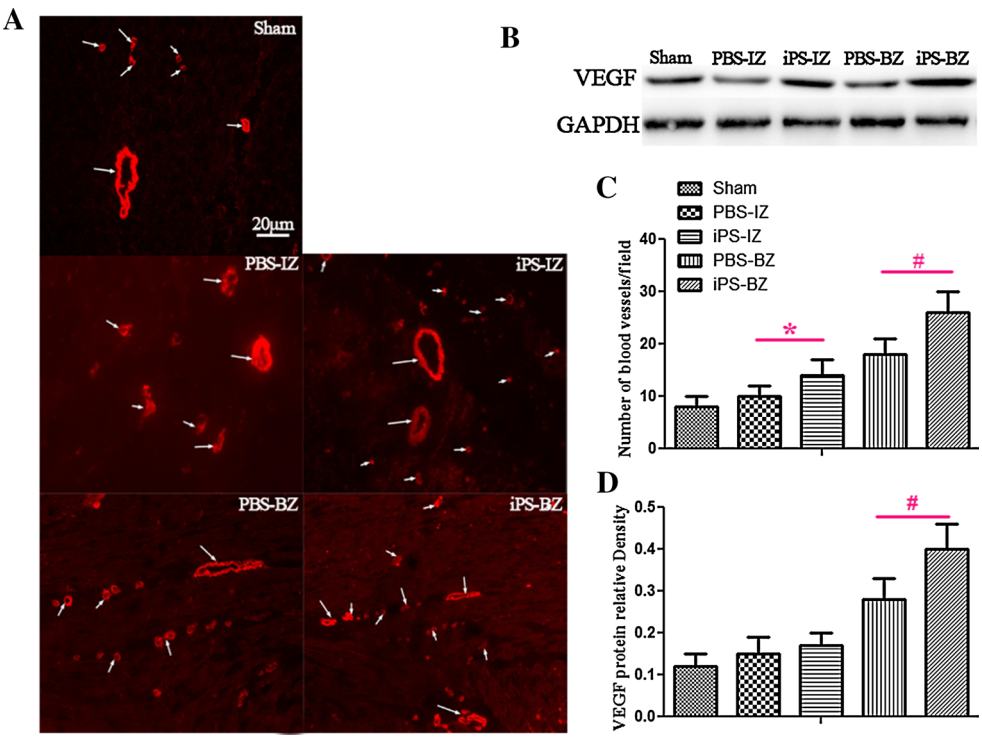

Fig. 4 Patterns of vascularization in different regions for each group. The fluorescence due to SMA antibody staining demonstrated that blood vessels were increased in iPS-treated hearts compared to PBS-treated hearts whether in IZ or BZ, as shown at the *red arrows* (**a**). Quantification of the new blood vessels indicated a clear increase in the iPSc group (**c**) (*iPS-IZ vs. PBS-IZ, # iPS-BZ vs. PBS-BZ, $P < 0.05$). Western blot analysis showed a significant increase in the expression of VEGF in the iPS-treated hearts compared with the PBS-treated hearts (**b**). Quantitative analyses of VEGF Western blot (**d**) (# iPS-BZ vs. PBS-BZ, $P < 0.05$). Magnification, ×200 for **a** (Color figure online)

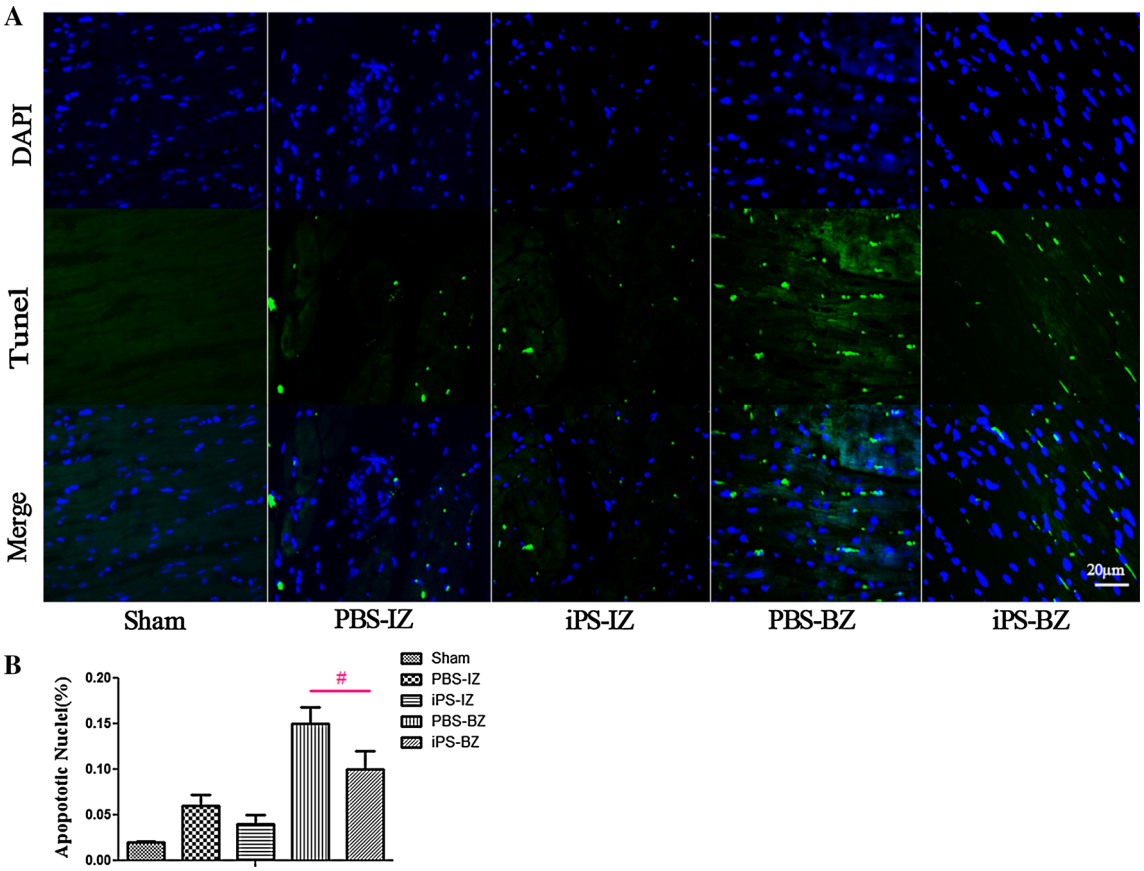

Fig. 5 iPSc transplantation on myocardial apoptosis. Representative tunel-staining pictures in sham hearts, IZ, and BZ of MI hearts (**a**). Quantitative analyses of apoptosis index in different regions of all groups (**b**). *iPS-BZ vs. PBS-BZ, $P < 0.05$

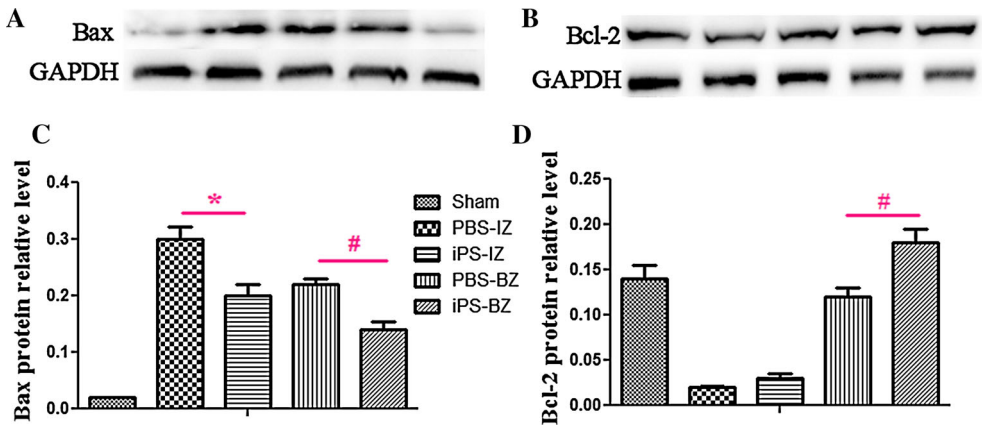

Fig. 6 The effect of iPSc transplantation on expression of antiapoptotic and proapoptotic proteins. iPSc transplantation significantly decreased the expression level of Bax compared with PBS group (**a**, **c**) (*iPS-IZ vs. PBS-IZ; #iPS-BZ vs. PBS-BZ, $P < 0.05$). iPSc transplantation significantly increased the expression level of Bcl-2 compared with PBS group (**b**, **d**) (#iPS-BZ vs. PBS-BZ, $P < 0.05$)

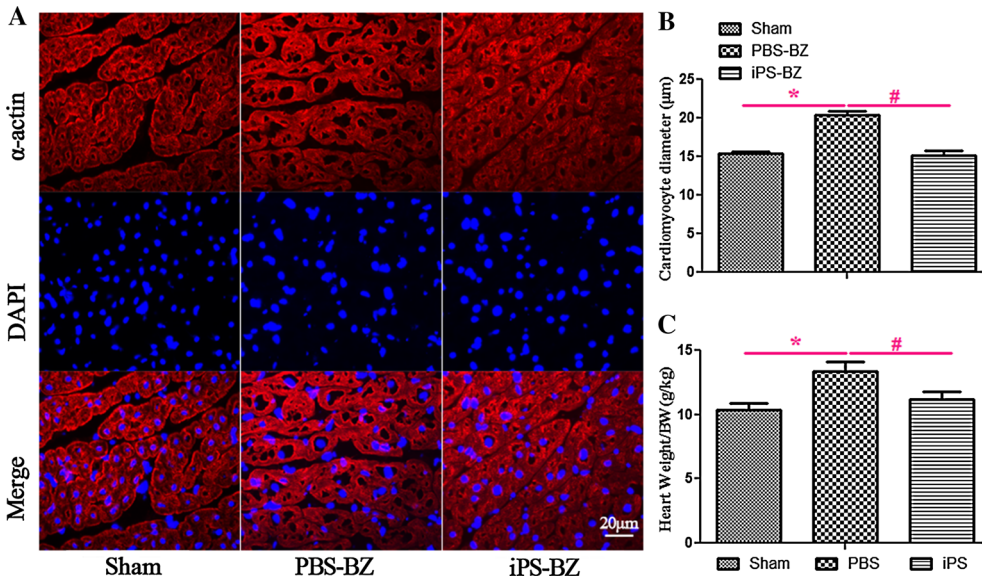

Fig. 7 iPS transplantation alleviates cardiomyocyte hypertrophy after MI. Representative picture of myocardial cell by immunofluorescence with actin antibody (**a**). Quantitative analyses of cardiomyocyte diameter (**b**) (*PBS-BZ vs. Shame-BZ; # iPS-BZ vs. PBS-BZ, $P < 0.05$). The WHW/BW in PBS group was significantly higher than Sham group, whereas the ratio was less in iPS group compared to PBS group (**c**) (*PBS group vs. Sham group; #iPS group vs. PBS group, $P < 0.05$)

Discussion

The emergence and development of induced pluripotent stem cells have been considered as the most significant recent achievements in life and medical science [5, 21]. In the present study, we injected undifferentiated iPSc into injured myocardium to investigate the therapeutic effects of this novel cell-based therapy in a post-infarcted swine model.

Regardless of stem cell type used for adoptive transfer therapy, substantial cell death after transplantation into the infarcted heart has been a significant impediment to initiate replacement or repair [22]. However, through the use of an immunofluorescence double-staining method, our research demonstrated that myocardial injected iPSc can persist in the infarction area and adapt to the host environment. This may be due to our use of an immunity inhibitor and glucocorticoids, which can improve the local milieu in acute MI and play a critical role in cell engraftment.

In accordance with previous study [14, 15], our results suggested transplantation of iPSc contributed to the functional improvement and infarct size limitation. However, the mechanism underlying cell-based therapeutic effects remains highly controversial all the time. Three general mechanisms have been proposed: transdifferentiation, cell fusion, and paracrine signaling [23]. To test whether the marked morphological and functional improvement were due to cardiac regeneration from the donor cells, we performed double staining for GFP and SMA on tissue frozen sections. However, functional cardiac fibers developed from donor cells could not be found on a large scale, and this extent of regeneration was relatively meager compared with the observed functional and structural improvement.

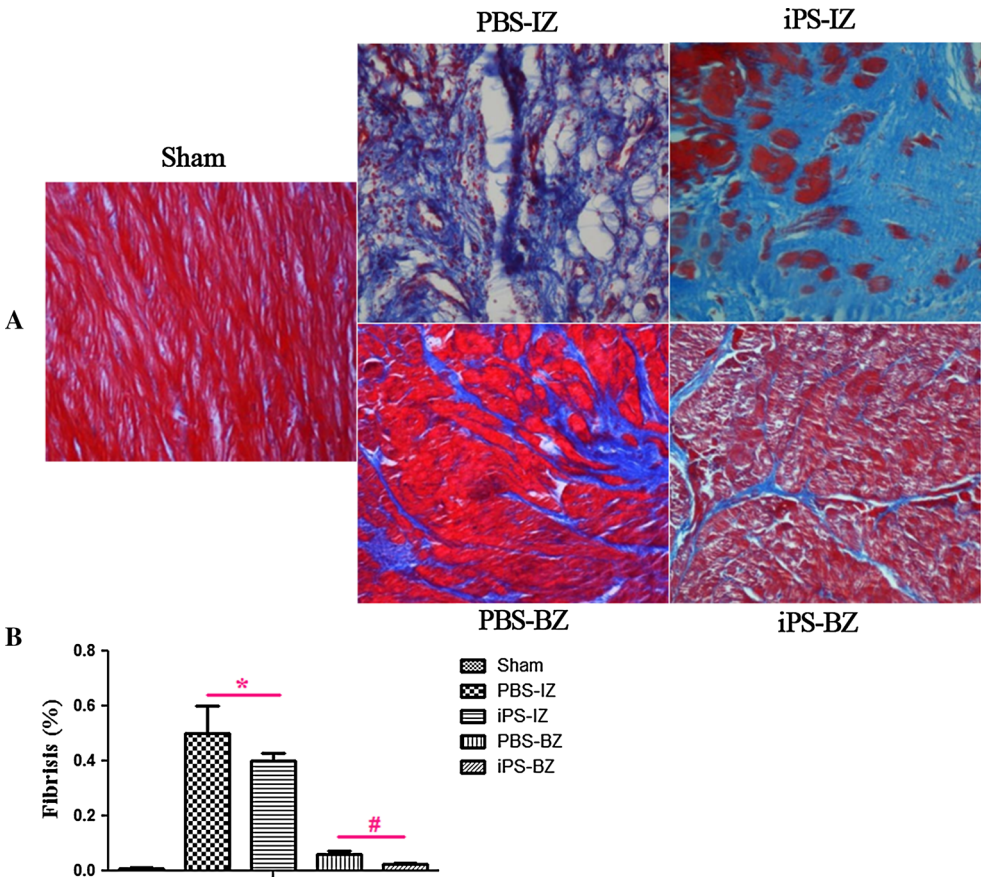

Fig. 8 iPS transplantation relieves myocardial fibrosis. Representative histological sections stained with Masson's trichrome (*blue stain*) in different regions from Sham, PBS, and iPS group (**a**). *Histogram* shows less fibrosis in the iPS group compared with the PBS group (**b**) (*iPS-IZ vs. PBS-IZ; #iPS-BZ vs. PBS-BZ, $P < 0.05$) (Color figure online)

Angiogenesis is a common mechanism of cell-based benefits, which has been demonstrated in bone marrow-derived multipotent progenitor cells for acute MI therapy [14] and iPSc for MI in a small animal model [24]. In this study, we also observed that the number of blood vessels in the iPS group was obviously higher than that in the PBS group, which could provide a basis for the protection afforded by iPSc injection. Our evidences indicated that transplanted iPSc differentiated to endothelial cells, or proper speaking, integrated into pre-existing vessels and to generate new vessel. Moreover, the level of VEGF was significantly elevated in iPS group compared with PBS group, suggesting a possible paracrine mechanism involved in the angiogenesis.

LV remodeling with myocardial apoptosis and hypertrophy occur to compensate for the loss of contracting myocardium after MI. Although stable LVEF may be maintained for a period of time, progressive myocardial dysfunction can develop and ultimately results in overt congestive heart failure (CHF). The mechanisms that contribute to the transition from the compensated state to CHF remain unclear but may be largely related to progressive contractile lesion in the border zone of infarct [25, 26]. Therefore, in this study, we observed the effect of iPSc transplantation on angiogenesis, cardiac apoptosis, fibrosis, and hypertrophy not only in the infracted zone but also in the border zone.

Apoptosis has been demonstrated to be a pivotal factor in the development and progression of post-MI remodeling that can lead to congestive heart failure [27]. The inhibition of apoptosis has been link to improvement of cardiac performance [27, 28]. In the present study, our evidences indicated that apoptosis of the host myocardium confirmed by TUNEL staining was significantly reduced in the iPSc-treated hearts. To investigate the underlying molecular mechanism of the antiapoptotic effects of iPS transplantation, we examined expression of the Bcl-2 protein family. The results suggested that expression of antiapoptotic proteins Bcl-2 was significantly increased in the iPS-treated hearts after MI compared with the PBS-treated hearts, while the proapoptotic proteins Bax was significantly decreased. Therefore, a reduction in post-MI apoptosis of the native cardiomyocytes is a general mechanism by which cellular transplantation post-MI exerts its beneficial effects.

In addition, adverse cardiac remodeling post-MI involves fibroblast proliferation, collagen deposition, and cardiomyocytes hypertrophy [29–31]. In this study, we

have shown that collagen deposition and cardiomyocyte diameter were significantly reduced by the following iPS cell transplantation in the infarcted heart, demonstrating an inhibition of cardiac fibrosis and cardiomyocyte hypertrophy, which seems to parallel the effects observed in stem cell studies previously [32, 33]. Therefore, reduction in fibrosis and attenuation in cardiomyocyte hypertrophy post-MI may be a shared mechanism by which iPSc transplantation exerts its potential therapeutic benefits, such as improved cardiac function and reduced scar size.

Our current studies, together with previous work performed in the rodent model [13–15], suggested that promotion of angiogenesis, as well as inhibition of apoptosis and fibrosis contributed to the improved cardiac function following transplantation of iPS cells. These effects may be more important than the actual replacement of injured cardiomyocytes by the transplanted iPSc, which were not provided in large enough numbers to replace the damaged cells. In spite of the original intention, we have demonstrated that direct transdifferentiation of iPSc into cardiomyocytes or fusion with host cardiomyocytes to replace or repair damaged myocardium, respectively, seems to be a quantitatively insignificant part of the limited process of repair. It appears that iPSc modify the local microenvironment by elaboration of autocrine or paracrine factors that encourage angiogenesis and survival, which limits inflammation. Expression of these and other yet unidentified factors may explain the capacity of iPSc to promote survival and proliferation of endogenous cells [34], including angiogenesis, inhibition of apoptosis, and fibrosis.

In summary, our study demonstrated that iPSc transplantation restored cardiac function by promoting angiogenesis and ameliorating adverse cardiac remodeling in a chronic post-infarcted swine model. The amelioration of cardiac remodeling in peri-infarct zone by iPSc transplantation was characterized by normalization of cardiac apoptosis, myocardial fibrosis, cardiomyocyte hypertrophy, and cardioprotective proteins expression. These findings may provide a basis for an autologous iPSc-based therapy of MI. However, future studies are warranted to determine whether these beneficial effects are due to the released factors from iPSc in vitro. Besides, the most important thing is to enhance the directional differentiation of iPS cells and realize effective myocardial regeneration on a large scale in vivo.

Acknowledgments This work was supported by grants from the National Natural Science Foundation of China (Grant Nos. 81170160, 30871077, 30800464).

References

1. Quijada, P., Toko, H., Fischer, K. M., Bailey, B., Reilly, P., Hunt, K. D., et al. (2012). Preservation of myocardial structure is enhanced by pim-1 engineering of bone marrow cells. *Circulation Research, 111*, 77–86.
2. Takemura, G., & Fujiwara, H. (2004). Role of apoptosis in remodeling after myocardial infarction. *Pharmacology and Therapeutics, 104*, 1–16.
3. Pfeffer, M. A., & Braunwald, E. (1990). Ventricular remodeling after myocardial infarction. Experimental observations and clinical implications. *Circulation, 81*, 1161–1172.
4. Foo, R. S., Mani, K., & Kitsis, R. N. (2005). Death begets failure in the heart. *Journal of Clinical Investigation, 115*, 565–571.
5. Yamanaka, S. (2007). Strategies and new developments in the generation of patient-specific pluripotent stem cells. *Cell Stem Cell, 1*, 39–49.
6. Nishikawa, S., Goldstein, R. A., & Nierras, C. R. (2008). The promise of human induced pluripotent stem cells for research and therapy. *Nature Reviews Molecular Cell Biology, 9*, 725–729.
7. Haase, A., Olmer, R., Schwanke, K., Wunderlich, S., Merkert, S., Hess, C., et al. (2009). Generation of induced pluripotent stem cells from human cord blood. *Cell Stem Cell, 5*, 434–441.
8. Mauritz, C., Schwanke, K., Reppel, M., Neef, S., Katsirntaki, K., Maier, L. S., et al. (2008). Generation of functional murine cardiac myocytes from induced pluripotent stem cells. *Circulation, 118*, 507–517.
9. Narazaki, G., Uosaki, H., Teranishi, M., Okita, K., Kim, B., Matsuoka, S., et al. (2008). Directed and systematic differentiation of cardiovascular cells from mouse induced pluripotent stem cells. *Circulation, 118*, 498–506.
10. Schenke-Layland, K., Rhodes, K. E., Angelis, E., Butylkova, Y., Heydarkhan-Hagvall, S., Gekas, C., et al. (2008). Reprogrammed mouse fibroblasts differentiate into cells of the cardiovascular and hematopoietic lineages. *Stem Cells, 26*, 1537–1546.
11. Olmer, R., Haase, A., Merkert, S., Cui, W., Palecek, J., Ran, C., et al. (2010). Long term expansion of undifferentiated human iPS and ES cells in suspension culture using a defined medium. *Stem Cell Research, 5*, 51–64.
12. Zweigerdt, R., Olmer, R., Singh, H., Haverich, A., & Martin, U. (2011). Scalable expansion of human pluripotent stem cells in suspension culture. *Nature Protocols, 6*, 689–700.
13. Singla, D. K., Long, X., Glass, C., Singla, R. D., & Yan, B. (2011). Induced pluripotent stem (iPS) cells repair and regenerate infarcted myocardium. *Molecular Pharmaceutics, 8*, 1573–1581.
14. Mauritz, C., Martens, A., Rojas, S. V., Schnick, T., Rathert, C., Schecker, N., et al. (2011). Induced pluripotent stem cell (iPSC)-derived Flk-1 progenitor cells engraft, differentiate, and improve heart function in a mouse model of acute myocardial infarction. *European Heart Journal, 32*, 2634–2641.
15. Nelson, T. J., Martinez-Fernandez, A., Yamada, S., Perez-Terzic, C., Ikeda, Y., & Terzic, A. (2009). Repair of acute myocardial infarction by human stemness factors induced pluripotent stem cells. *Circulation, 120*, 408–416.
16. Wu, Z., Chen, J., Ren, J., Bao, L., Liao, J., Cui, C., et al. (2009). Generation of pig induced pluripotent stem cells with a drug-inducible system. *Journal of Molecular Cell Biology, 1*, 46–54.
17. Yang, Y. J., Qian, H. Y., Huang, J., Li, J. J., Gao, R. L., Dou, K. F., et al. (2009). Combined therapy with simvastatin and bone marrow-derived mesenchymal stem cells increases benefits in infarcted swine hearts. *Arteriosclerosis, Thrombosis, and Vascular Biology, 29*, 2076–2082.
18. Li, C., Tang, L., Yang, Z., & Cao, K. (2011). Integration of dual source computed tomography with magnetic navigation system for percutaneous coronary intervention: a feasibility study. *Catheterization and Cardiovascular Interventions, 78*, 1108–1115.
19. Zhang, S., Ge, J., Zhao, L., Qian, J., Huang, Z., Shen, L., et al. (2007). Host vascular niche contributes to myocardial repair induced by intracoronary transplantation of bone marrow CD34+

progenitor cells in infarcted swine heart. *Stem Cells, 25*, 1195–1203.
20. Zhang, Z., Li, S., Cui, M., Gao, X., Sun, D., Qin, X., et al. (2013). Rosuvastatin enhances the therapeutic efficacy of adipose-derived mesenchymal stem cells for myocardial infarction via PI3 K/Akt and MEK/ERK pathways. *Basic Research in Cardiology, 108*, 333.
21. Yu, J., Vodyanik, M. A., Smuga-Otto, K., Antosiewicz-Bourget, J., Frane, J. L., Tian, S., et al. (2007). Induced pluripotent stem cell lines derived from human somatic cells. *Science, 318*, 1917–1920.
22. Menasche, P. (2004). Cellular transplantation: hurdles remaining before widespread clinical use. *Current Opinion in Cardiology, 19*, 154–161.
23. Amado, L. C., Saliaris, A. P., Schuleri, K. H., St John, M., Xie, J. S., Cattaneo, S., et al. (2005). Cardiac repair with intramyocardial injection of allogeneic mesenchymal stem cells after myocardial infarction. *Proceedings of the National Academy of Sciences of the USA, 102*, 11474–11479.
24. Yan, B., Abdelli, L. S., & Singla, D. K. (2011). Transplanted induced pluripotent stem cells improve cardiac function and induce neovascularization in the infarcted hearts of db/db mice. *Molecular Pharmaceutics, 8*, 1602–1610.
25. Bolognese, L., Neskovic, A. N., Parodi, G., Cerisano, G., Buonamici, P., Santoro, G. M., et al. (2002). Left ventricular remodeling after primary coronary angioplasty: Patterns of left ventricular dilation and long-term prognostic implications. *Circulation, 106*, 2351–2357.
26. Hu, Q., Wang, X., Lee, J., Mansoor, A., Liu, J., Zeng, L., et al. (2006). Profound bioenergetic abnormalities in peri-infarct myocardial regions. *American Journal of Physiology Heart and Circulatory Physiology, 291*, 648–657.
27. Kumar, D., & Jugdutt, B. I. (2003). Apoptosis and oxidants in the heart. *Journal of Laboratory and Clinical Medicine, 142*, 288–297.
28. Kumar, D., Lou, H., & Singal, P. K. (2002). Oxidative stress and apoptosis in heart dysfunction. *Herz, 27*, 662–668.
29. Jugdutt, B. I. (2003). Remodeling of the myocardium and potential targets in the collagen degradation and synthesis pathways. *Current Drug Targets: Cardiovascular and Haematological Disorders, 3*, 1–30.
30. Jugdutt, B. I. (2003). Ventricular remodeling after infarction and the extracellular collagen matrix: When is enough enough. *Circulation, 108*, 1395–1403.
31. Jugdutt, B. I., Menon, V., Kumar, D., & Idikio, H. (2002). Vascular remodeling during healing after myocardial infarction in the dog model: Effects of reperfusion, amlodipine and enalapril. *Journal of the American College of Cardiology, 39*, 1538–1545.
32. Fatma, S., Selby, D. E., Singla, R. D., & Singla, D. K. (2010). Factors Released from Embryonic Stem Cells Stimulate c-kit-FLK-1(+ve) Progenitor Cells and Enhance Neovascularization. *Antioxidants and Redox Signaling, 13*, 1857–1865.
33. Singla, D. K., Lyons, G. E., & Kamp, T. J. (2007). Transplanted embryonic stem cells following mouse myocardial infarction inhibit apoptosis and cardiac remodeling. *American Journal of Physiology Heart and Circulatory Physiology, 293*, 1308–1314.
34. Xiong, Q., Ye, L., Zhang, P., Lepley, M., Swingen, C., Zhang, L., et al. (2012). Bioenergetic and functional consequences of cellular therapy: activation of endogenous cardiovascular progenitor cells. *Circulation Research, 111*, 455–468.